Article (refereed) – Published version

The importance of shallow hydrothermal island arc systems in ocean biogeochemistry

Jeffrey A. Hawkes[1,2], Douglas P. Connelly[3], Micha J. A. Rijkenberg[4], and Eric P. Achterberg[1,5]

[1]Ocean and Earth Science, NOCS, University of Southampton, Southampton, UK, [2]Now at ICBM, Universität Oldenburg, Oldenburg, Germany, [3]National Oceanography Centre Southampton, Southampton, UK, [4]Royal Netherlands Institute for Sea Research, Den Burg, Netherlands, [5]Now at GEOMAR, Helmholtz Centre for Ocean Research, Kiel, Germany

Abstract Hydrothermal venting often occurs at submarine volcanic calderas on island arc chains, typically at shallower depths than mid–ocean ridges. The effect of these systems on ocean biogeochemistry has been under-investigated to date. Here we show that hydrothermal effluent from an island arc caldera was rich in Fe(III) colloids (0.02–0.2 μm; 46% of total Fe), contributing to a fraction of hydrothermal Fe that was stable in ocean water. Iron(III) colloids from island arc calderas may be transferred into surrounding waters (generally 0–1500 m depth) by ocean currents, thereby potentially stimulating surface ocean primary productivity. Hydrothermal Fe oxyhydroxide particles (>0.2 μm) were also pervasive in the studied caldera and contained high concentrations of oxyanions of phosphorus (P), vanadium (V), arsenic (As), and manganese (Mn). Hydrothermal island arcs may be responsible for >50% of global hydrothermal P scavenging and >40% V scavenging, despite representing <10% of global hydrothermal fluid flow.

1. Introduction

Submarine island arc seamounts and calderas often host hydrothermal activity [*de Ronde et al.*, 2001; *Baker et al.*, 2008] and account for ~9% of global hydrothermal water fluxes [*Baker et al.*, 2008]. Calderas can trap effluent material [*Staudigel et al.*, 2004], and overturning of caldera water through breaches in the rim and by vertical mixing allows the accumulated hydrothermal material to periodically or continually enter into the ocean, allowing large chemical and heat fluxes from island arc systems [*Staudigel et al.*, 2004].

Usually the vent fluids at island arcs are rich in total sulfur and are highly acidic due to the direct degassing of magma-derived SO_2 and CO_2 [*Butterfield et al.*, 2011; *Resing et al.*, 2007; *de Ronde et al.*, 2011], and this high acidity leads to elevated iron (Fe) levels in the resulting hydrothermal plumes [*Resing et al.*, 2007; *Leybourne et al.*, 2012]. Iron is a critical micronutrient for ocean productivity, and inputs from deep ocean (>2000 m) hydrothermal vents strongly influence the global distribution of Fe [*Tagliabue et al.*, 2010]. Shallower (typically <1500 m) island arc hydrothermal activity has received less attention for its role in ocean biogeochemistry, even though several island arcs occur in high-latitude settings (Figure 1a) where low Fe levels often limit primary productivity [*Nielsdóttir et al.*, 2012].

Hydrothermal activity plays a critical role in the chemical composition of the ocean through high temperature alteration of seawater and scavenging of dissolved elements with Fe oxyhydroxides in hydrothermal plumes. These effects are potentially different at island arcs due to the greater influence of magmatic gases and acidity [*Butterfield et al.*, 2011; *Resing et al.*, 2007] and the consequences of this for ocean chemistry are under-investigated. In this study, we investigated the speciation of hydrothermal Fe and the scavenging of dissolved oxyanions in an island arc caldera in the Southern Ocean.

2. Methods

2.1. Study Area

The Kemp Caldera is on the South Sandwich island arc in the eastern Scotia Sea of the Southern Ocean (Figure 1). The caldera floor is 1600 m deep, and the rim has a diameter of ~7 km at an average 814 m depth. A resurgent cone rising ~250 m from the base hosted vents with sulfide rich hydrothermal fluids. Here we present data from two cruises aboard the RRS *James Cook*: JC042 in February 2010 and JC055 in February 2011.
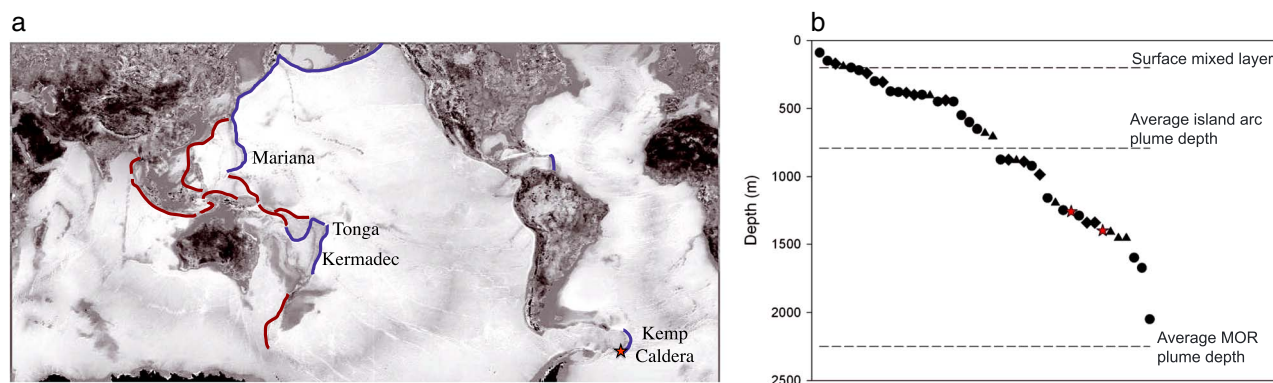
Figure 1. Island arc locations and their plume depths. (a) Location of the Kemp Caldera on the South Sandwich island arc, and other island arcs systems, which mainly occur in the western Pacific Ocean [after *Baker et al.*, 2008]. Island arcs that are predominantly subaerial are shown as red lines and those predominantly submarine as blue lines. (b) Depths of island arc hydrothermal plumes from the Mariana Arc (circles) [*Resing et al.*, 2009], Kermadec Arc (triangles) [*de Ronde et al.*, 2001], Tonga Arc (diamonds) [*Massoth et al.*, 2007] and Kemp Caldera (red stars), compared with average mid–ocean ridge (MOR) plume depth and typical oceanic surface mixed layer depth [*de Boyer Montégut et al.*, 2004].

2.2. Sample Collection and Analysis

Samples were taken for particulate ($>0.2\,\mu m$), dissolved ($<0.2\,\mu m$) and soluble ($<0.02\,\mu m$) concentrations of metals and oxyanions using externally sprung 10 L Teflon-lined Ocean Test Equipment water sampling bottles and a Seabird +911 conductivity-temperature-depth (CTD) profiler system, all mounted on a titanium frame. The CTD profiler was equipped with a light scattering sensor (LSS) and reductive potential (Eh) detector.

Particulate concentrations of metals and oxyanions were measured by Inductively Coupled Plasma–Mass Spectrometry (ICP-MS; Thermo Scientific X-series) after digestion in nitric acid for 3 days at 150°C. Metal concentrations in acidified seawater were measured after buffering to pH 7.5–8.5, equilibration with 2% weight per volume (w/v) ammonium 1-pyrrolidine dithiocarbamate and 2% w/v diethyldithiocarbamic acid, liquid extraction into chloroform, drying, dissolution in 3% nitric acid and analysis by ICP-MS (Thermo Scientific X-series). Labile dissolved Fe (DFe) was measured in several filtered, frozen samples by overnight equilibration with 1-nitroso-2-naphthol after defrosting and analysis by adsorptive cathodic stripping voltammetry [*Hawkes et al.*, 2013]. Dissolved inorganic carbon and alkalinity were measured using a Versatile Instrument for the Determination of Titration Alkalinity 3C analyzer (Miranda). Nutrients (phosphate and silicate) were measured by Seal QuAAtro, and these data were used to calculate in situ pH [*Lewis et al.*, 1998].

3. Results and Discussion

3.1. Metal Concentrations and Sources in the Kemp Caldera

Enhanced concentrations of Fe and Mn were found at two stations within the caldera, at concentrations up to 100 times higher than typical levels at similar depths in the Southern Ocean [*Bucciarelli et al.*, 2001; *Nielsdóttir et al.*, 2012] (Figure 2). The "Hydrothermal" station was sampled over an active vent field, with highly sulfidic and Mn rich fluids. This vent field supplied two hydrothermal plumes (Figure 2c; 1400 m and 1260 m depth), as indicated by the LSS profile. These plumes were accompanied by temperature anomalies (+0.4 and +0.2°C, respectively), increases in reductive potential (lower Eh) and increased Mn concentrations, but not increased Fe, during two consecutive years of sampling (Figure 2). The second station (Mid-caldera) was ~ 2 km away from the discovered vent field, over the deepest part of the caldera (Figure 2). Here Fe concentrations were similar to those in the hydrothermal station plumes at similar depths, suggesting that an undiscovered vent site had supplied the high levels of Fe throughout the caldera. It is also possible that before 2010 the vent fluids on the resurgent cone were significantly more Fe rich and that the Fe phases in the caldera are stable on these timescales.

A third, shallower particle plume (~1000 m depth) was present at both stations and was variable in magnitude over several CTD casts. This plume had no hydrothermal anomalies (other than LSS signal) and may be due to a nonhydrothermal process such as sediment resuspension from the sill of the caldera [*Leybourne et al.*, 2012].
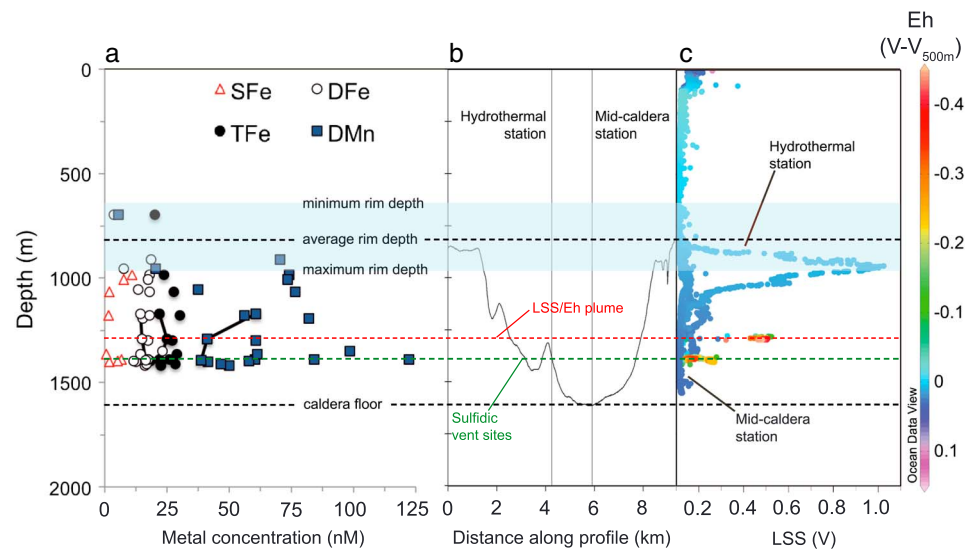
Figure 2. Depth profiles of physical and chemical variables for the Kemp Caldera. (a) Mn and Fe (total; TFe, dissolved; DFe, and soluble; SFe) concentrations with depth. The data points from the background station are connected by a black line. All other points are from several casts at the hydrothermal station. (b) Bathymetry of the Caldera with the resurgent cone shown at 4 km along the profile displayed (bathymetry 8 times vertically exaggerated). (c) Light scattering sensor (LSS) voltage signals at the hydrothermal and mid-caldera stations with Eh (reductive potential) anomaly indicated by color. The Eh readings are normalized to the 500 m value to correct for detector drift. The depth of the caldera floor, rim minimum, maximum, and average are indicated, external water can breach the caldera at the deeper parts of the rim and flush hydrothermally influenced water into the Southern Ocean.

Hydrothermal island arcs often host hot fluids at several sites with highly variable water/rock reaction dynamics, resulting in varying sulfur chemistry, acidity, and gas concentration in the fluids [*de Ronde et al.*, 2011; *Leybourne et al.*, 2012]. The type of low Fe, high Mn, and high sulfur system sampled at the vent field on the resurgent cone flank is typical of systems with very long water/rock reaction pathways, and shorter pathways typically lead to high Fe and acid/gas-rich vent fluids [*de Ronde et al.*, 2011; *Leybourne et al.*, 2012; *Resing et al.*, 2007]. Here we assume that the Fe in the Kemp caldera is supplied by a short water/rock reaction system within the caldera. The total Fe:Mn ratios observed inside the caldera varied between a background of ~0.58 to a low figure of ~0.21 with increasing influence (addition of Mn) from the resurgent cone flank fluids (Fe:Mn < 0.01) (Figure 3). Ratios of Fe:Mn up to 14 have been found in acidic, gaseous fluids at island arcs [*de Ronde et al.*, 2011], and it may be possible in future campaigns to estimate the proportion of total hydrothermal Fe (dissolved or total) that remains in an island arc given similar ratio analysis.

Almost all Mn in the caldera was in the dissolved phase (97.0 ± 3.3%, mean ± 1 standard deviation) due to its longer oxidation rate in hydrothermal plumes [*Rudnicki and Elderfield*, 1993], whereas Fe was partitioned between soluble (<0.02 μm), colloidal (0.02–0.2 μm), and particulate (>0.2 μm) phases in fractions averaging 19 ± 15%, 46 ± 15% and 35 ± 12%, respectively (mean ± 1 standard deviation). A highly variable portion (9.7–82.2%), but typically about 5 nM, of DFe occurred as "labile" Fe (see section 2; Figure 3), indicating that some Fe was

Figure 3. Fe concentrations versus Mn concentration in and outside the Kemp Caldera. Ratios of Fe:Mn are shown as a guide. The focused fluids sampled from the resurgent cone had an Fe:Mn ratio of <0.01, suggesting that a higher Fe:Mn hydrothermal fluid source exists in the caldera. Fluids with Fe:Mn up to 14 have been sampled at other acidic hydrothermal island arcs [*de Ronde et al.*, 2011].
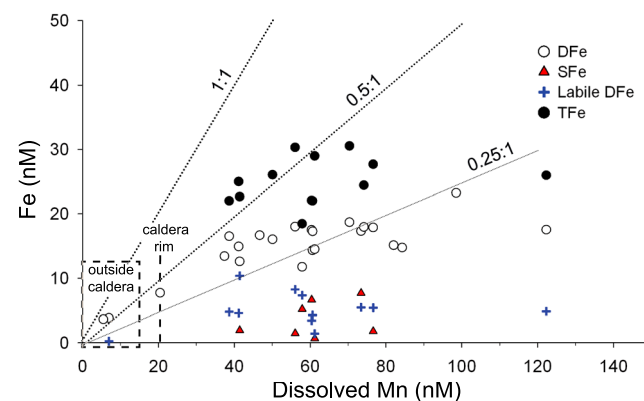
Table 1. Particulate Phase Relationships Between Scavenged Species and Fe

	P_{Ox}:Fe	V_{Ox}:Fe	As_{Ox}:Fe	Mn:Fe
Molar ratio	0.41	0.0046	0.0013	0.16
R^2	0.83	0.87	0.49	0.67
N	12	16	16	16
P value	<0.001	<0.001	0.002	<0.001
Predicted molar ratio[a]	0.17	0.0032	-	-

[a]Predicted from dissolved phosphate concentration of 2.44 μM [*Edmonds and German*, 2004].

bound to weak organic ligands ($\log K'_{FeL} < 23$) or weakly crystalline mineral phases [*Hawkes et al.*, 2013]. This "labile" portion was unrelated to the total Fe concentration, probably indicating a variable degree of crystallinity and reactivity of Fe-oxyhydroxide and ligand phases [*Anschutz and Penn*, 2005]. Iron-rich particles were pervasive at both hydrothermal and mid-caldera stations, and the fractions of oxyanions P_{Ox}, V_{Ox} and As_{Ox}, and Mn covaried with Fe in the particles in ratios 0.41, 0.0046, 0.0013, and 0.16, respectively (Table 1). The P_{Ox} and V_{Ox} to Fe ratios were considerably higher than those typically found (0.17 and 0.0032, respectively) in hydrothermal plume particles at similar dissolved phosphate concentrations [*Feely et al.*, 1998; *Edmonds and German*, 2004]; see supporting information. Manganese also correlated well with Fe in the particulate phase (Table 1), probably due to scavenging following adsorptive and bacterial oxidation of Mn [*Feely et al.*, 1996].

Iron oxyhydroxide colloids (0.02–0.2 μm) form in hydrothermal plumes following the oxidation of hydrothermal Fe(II) and form a precursor to Fe(III) particles (>0.2 μm), which settle and contribute to hydrothermal iron-rich sediments. In island arc plumes, where pH is reduced compared with mid–ocean ridge plumes as a result of the dissolution of magmatic SO_2 and CO_2 [*Resing et al.*, 2007], the rate of Fe(II) oxidation is decreased. This is critical in the partitioning of size fractions because dilution of soluble and colloidal Fe in the plume reduces the rate of aggregation to particulate Fe [*Field and Sherrell*, 2000; *Honeyman and Santschi*, 1989]. Sulfide is usually a minor component of acidic island arc vents [*Butterfield et al.*, 2011], where sulfite is the main sulfur species. Therefore, Fe sulfides make up a smaller proportion of plume particles compared with mid–ocean ridge plumes.

At the ambient temperature, $[O_2]$ and pH_{tot} (7.85) in the Kemp Caldera, and using the equations of *Millero et al.* [1987], the oxidation half-life of Fe(II) was ~0.9 h (see supporting information). This is comparable to the typical emplacement time of hydrothermal fluids to neutrally buoyant plume height (~1 h), where ~10,000 times dilution of the fluid has occurred [*Field and Sherrell*, 2000]. At lower pH (7.75, 7.55, and 6.85), typical of island arc plumes [*Leybourne et al.*, 2012; *Resing et al.*, 2007], the half-life increases to ~1.4 h, ~3.4 h and ~86 h, respectively. The slow formation of Fe oxides along with their continual dilution in the plume leads to the domination of colloidal over particulate sized Fe oxyhydroxides in the Kemp Caldera, and generally suggests that a higher proportion of island arc hydrothermal Fe will be stable in ocean waters than at mid–ocean ridges.

3.2. Island Arc and Global Hydrothermal Plume Removal of Dissolved P and V

The oxyanions of P, V, and U are depleted in vent fluids [*Edmonds and German*, 2004; *Wheat et al.*, 1996], and are further removed from ocean water onto oxyhydroxide particles [*Edmonds and German*, 2004]. The increased surface area and longevity of the colloidal Fe-oxyhydroxide phases, which aggregate to form particles, likely

Table 2. Global Average Data for Calculation of Dissolved Oxyanion Removal by Hydrothermal Plumes

	Island Arc	Mid–Ocean Ridge/ Back-Arc Basin	Global Hydrothermal (% River)	Global River
Global fluid flow (kg yr^{-1})[a]	4.73×10^{12}	4.53×10^{13}	5×10^{13} (0.13%)	3.74×10^{16}
Fe oxyhydroxides per kg fluid (mmol)[b]	2.45	0.5	0.7	-
P:Fe[c]	0.41	0.16	0.18	-
V:Fe[c]	0.0046	0.0032	0.0033	-
P flux[d] (10^{10} mol yr^{-1})	−0.48	−0.36	0.84 (30%)	3.00
V flux[d] (10^8 mol yr^{-1})	−0.53	−0.72	1.26 (25%)	5.00

[a]Hydrothermal flux [*Nielsen et al.*, 2006; *Palmer and Edmond*, 1989]. Island arc percent [*Baker et al.*, 2008]. Global river flux [*Palmer and Edmond*, 1989].
[b]Island arcs [*Butterfield et al.*, 2011; *de Ronde et al.*, 2011], axial sites [*Hawkes et al.*, 2013]. We approximate that 50% of all hydrothermal Fe forms oxyhydroxides in both environments [*de Ronde et al.*, 2011; *Field and Sherrell*, 2000].
[c]*Feely et al.* [1998].
[d]*Wheat et al.* [1996] and *Trefry and Metz* [1989].

enhanced scavenging of oxyanions, as scavenging proceeds faster than aggregation of precipitates [*Rudnicki and Elderfield*, 1993]. If our particulate oxyanion concentrations are typical in island arc hydrothermal oxyhydroxide precipitates, and not accounting for (unknown) temporal variability, we can estimate the global importance of this scavenging effect. We used the estimated global average Fe, P and V hydrothermal and fluvial flux data and their hydrothermal elemental ratios (Table 2) to find that island arc hydrothermal plumes scavenge 0.48×10^{10} mol P yr^{-1} and 0.53×10^8 mol V yr^{-1}, while the rest of the ridge systems scavenge 0.36×10^{10} mol yr^{-1} and 0.72×10^8 mol yr^{-1}, respectively. These values compare with river inputs of dissolved P and V of 3.0×10^{10} mol yr^{-1} and 5.0×10^8 mol yr^{-1}, respectively, and so hydrothermal plumes may remove 30% and 25% of dissolved river P and V, respectively—with island arcs contributing 57% and 42% of the global hydrothermal removal, respectively, despite only representing 9.4% of the total global hydrothermal fluid discharge. Some of these phases may be remineralized during oxic sediment diagenesis [*Poulton and Canfield*, 2006], but those present as colloids are likely to represent a long term sink of oxyanions from the truly dissolved phase.

3.3. Hydrothermal Island Arc Provision of DFe to Surface Waters

Iron is a limiting or colimiting micronutrient in many oceanic surface waters [*Nielsdóttir et al.*, 2012] and Fe colloids can be bioavailable to microorganisms [*Nodwell and Price*, 2001]. Indeed, our experiments showed that a large portion of DFe in this caldera was chemically labile to exchange with an added ligand (Figure 3), and this may be due to the presence of fresh, amorphous hydrothermal colloids [*Hawkes et al.*, 2013]. The transfer of colloidal DFe from hydrothermal island arc calderas to the surface ocean may therefore be important in ocean fertilization.

Iron and Mn concentrations in the caldera were similar in 2010 and 2011, suggesting that vent inputs and losses from the caldera were well balanced over this time period. Using CTD data and "Thorpe scales", we calculated an average vertical diffusivity (K_z) of 1.14×10^{-4} m^2 s^{-1} between the depths of 1000 m to 695 m over the Kemp Caldera (see supporting information). The gradient in concentration of Mn and Fe over these depths was 192.4 and 41.1 nmol m^{-4}, respectively, and the resultant loss flux by vertical diffusion over the entire rim area (3.9×10^7 m^2) of the caldera was 74.0 and 15.8 mol d^{-1}, respectively. A typical vent field fluxes ~150 kg s^{-1} vent fluid [*Baker et al.*, 1993], containing ~1 mM Fe and Mn, and can therefore flux >10,000 mol d^{-1} Fe and Mn, and loss by vertical diffusion can therefore only explain <1% of the hydrothermal inputs. This suggests that horizontal displacement through breaches in the caldera rim [*Staudigel et al.*, 2004] was more important than turbulent vertical diffusion in the transport of metals away from this system. We cannot calculate the scale of transport of DFe out of this caldera compared with precipitation and settling to sediments, but the low concentration and small size of the Fe colloids greatly reduces the chance of further aggregation [*Honeyman and Santschi*, 1989] and settling [*Yücel et al.*, 2011], respectively, and suggests that these environments are important sources of DFe to surrounding waters. This is particularly the case for island arc hydrothermal vents that are not constrained by high-sided calderas, where hydrothermal material can be freely transported into the surrounding waters.

Shallow island arc vent plumes may therefore supply Fe that reaches surface ocean photosynthetic communities. The supplies include more labile, fresher material than the hydrothermal input reaching surface waters from deep ocean systems [*Tagliabue et al.*, 2010], and may be more consistent and less periodic or climate dependent than other sources of Fe to the surface ocean, such as dust deposition or sea ice [*Tagliabue et al.*, 2010]. The Kemp Caldera forms an important source of Fe but may be too deep to directly fertilize its overlying surface ocean ecosystems (Figure 1b). Many other hydrothermal plumes along global island arcs are shallower than the typical surface mixed layer depth (typically <150 m; [*de Boyer Montégut et al.*, 2004]), and will therefore directly influence ocean productivity, particularly at high latitudes where the mixed layer depth is deeper [*de Boyer Montégut et al.*, 2004].

References

Anschutz, A. J., and R. L. Penn (2005), Reduction of crystalline iron III oxyhydroxides using hydroquinone: Influence of phase and particle size, *Geochem. Trans.*, 6(3), 60–66.

Baker, E. T., G. J. Massoth, S. L. Walker, and R. W. Embley (1993), A method for quantitatively estimating diffuse and discrete hydrothermal discharge, *Earth Planet. Sci. Lett.*, 118(1), 235–249.

Baker, E. T., R. W. Embley, S. L. Walker, J. A. Resing, J. E. Lupton, K.-I. Nakamura, C. E. J. de Ronde, and G. J. Massoth (2008), Hydrothermal activity and volcano distribution along the Mariana arc, *J. Geophys. Res.*, 113, B08S09, doi:10.1029/2007JB005423.

Bucciarelli, E., S. Blain, and P. Tréguer (2001), Iron and manganese in the wake of the Kerguelen Islands (Southern Ocean), *Mar. Chem.*, *73*(1), 21–36.

Butterfield, D. A., K.-I. Nakamura, B. Takano, M. D. Lilley, J. E. Lupton, J. A. Resing, and K. K. Roe (2011), High SO$_2$ flux, sulfur accumulation, and gas fractionation at an erupting submarine volcano, *Geology*, *39*(9), 803–806.

de Boyer Montégut, C., G. Madec, A. S. Fischer, A. Lazar, and D. Iudicone (2004), Mixed layer depth over the global ocean: An examination of profile data and a profile-based climatology, *J. Geophys. Res.*, *109*, C12003, doi:10.1029/2004JC002378.

de Ronde, C. E., et al. (2011), "Submarine hydrothermal activity and gold-rich mineralization at Brothers Volcano, Kermadec Arc, New Zealand", *Miner. Deposita*, *46*(5), 541–584.

de Ronde, C., E. Baker, G. Massoth, J. Lupton, I. Wright, R. Feely, and R. Greene (2001), Intra-oceanic subduction-related hydrothermal venting, Kermadec volcanic arc, New Zealand, *Earth Planet. Sci. Lett.*, *193*(3-4), 359–369.

Edmonds, H., and C. German (2004), Particle geochemistry in the Rainbow hydrothermal plume, Mid-Atlantic Ridge, *Geochim. Cosmochim. Acta*, *68*(4), 759–772.

Feely, R. A., J. H. Trefry, G. T. Lebon, and C. R. German (1998), The relationship between P/Fe and V/Fe ratios in hydrothermal precipitates and dissolved phosphate in seawater, *Geophys. Res. Lett.*, *25*(13), 2253–2256.

Feely, R., E. Baker, K. Marumo, T. Urabe, J. Ishibashi, J. Gendron, G. Lebon, and K. Okamura (1996), Hydrothermal plume particles and dissolved phosphate over the superfast-spreading southern East Pacific Rise, *Geochim. Cosmochim. Acta*, *60*(13), 2297–2323.

Field, M. P., and R. M. Sherrell (2000), Dissolved and particulate Fe in a hydrothermal plume at 9°45′N, East Pacific Rise: Slow Fe (II) oxidation kinetics in Pacific plumes, *Geochim. Cosmochim. Acta*, *64*(4), 619–628.

Hawkes, J. A., D. P. Connelly, M. Gledhill, and E. P. Achterberg (2013), The stabilisation and transportation of dissolved iron from high temperature hydrothermal vent systems, *Earth Planet. Sci. Lett.*, *375*, 280–290.

Honeyman, B. D., and P. H. Santschi (1989), A Brownian-pumping model for oceanic trace metal scavenging: Evidence from Th isotopes, *J. Mar. Res.*, *47*(4), 951–992.

Lewis, E., D. Wallace, and L. J. Allison (1998), Program developed for CO$_2$ system calculations (No. ORNL/CDIAC–105). Brookhaven National Lab., Dept. of Applied Science, Upton, N. Y.; Oak Ridge National Lab., Carbon Dioxide Information Analysis Center, Oak Ridge, Tenn.

Leybourne, M. I., et al. (2012), Submarine magmatic-hydrothermal systems at the Monowai Volcanic Center, Kermadec Arc, *Econ. Geol.*, *107*(8, SI), 1669–1694.

Massoth, G., et al. (2007), Multiple hydrothermal sources along the south Tonga arc and Valu Fa Ridge, *Geochem. Geophys. Geosyst.*, *8*, Q11008, doi:10.1029/2007GC001675.

Millero, F. J., S. Sotolongo, and M. Izaguirre (1987), The oxidation kinetics of Fe(II) in seawater, *Geochim. Cosmochim. Acta*, *51*(4), 793–801.

Nielsdóttir, M. C., T. S. Bibby, C. M. Moore, D. J. Hinz, R. Sanders, M. Whitehouse, R. Korb, and E. P. Achterberg (2012), Seasonal and spatial dynamics of iron availability in the Scotia Sea, *Mar. Chem.*, *130*, 62–72.

Nielsen, S. G., M. Rehkämper, D. A. Teagle, D. A. Butterfield, J. C. Alt, and A. N. Halliday (2006), Hydrothermal fluid fluxes calculated from the isotopic mass balance of thallium in the ocean crust, *Earth Planet. Sci. Lett.*, *251*(1), 120–133.

Nodwell, L. M., and N. M. Price (2001), Direct use of inorganic colloidal iron by marine mixotrophic phytoplankton, *Limnol. Oceanogr.*, *46*(4), 765–777.

Palmer, M. R., and J. M. Edmond (1989), The strontium isotope budget of the modern ocean, *Earth Planet. Sci. Lett.*, *92*(1), 11–26.

Poulton, S. W., and D. E. Canfield (2006), Co-diagenesis of iron and phosphorus in hydrothermal sediments from the southern East Pacific Rise: Implications for the evaluation of paleoseawater phosphate concentrations, *Geochim. Cosmochim. Acta*, *70*, 5883–5898.

Resing, J. A., E. T. Baker, J. E. Lupton, S. L. Walker, D. A. Butterfield, G. J. Massoth, and K.-I. Nakamura (2009), Chemistry of hydrothermal plumes above submarine volcanoes of the Mariana Arc, *Geochem. Geophys. Geosyst.*, *10*, Q02009, doi:10.1029/2008GC002141.

Resing, J., G. Lebon, E. Baker, J. Lupton, R. Embley, G. Massoth, W. Chadwick, and C. De Ronde (2007), Venting of acid-sulfate fluids in a high-sulfidation setting at NW Rota-1 submarine volcano on the Mariana Arc, *Econ. Geol.*, *102*(6), 1047–1061.

Rudnicki, M. D., and H. Elderfield (1993), A chemical-model of the buoyant and neutrally buoyant plume above the Tag Vent Field, 26°N, Mid-Atlantic Ridge, *Geochim. Cosmochim. Acta*, *57*(13), 2939–2957.

Staudigel, H., S. R. Hart, A. A. Koppers, C. Constable, R. Workman, M. Kurz, and E. T. Baker (2004), Hydrothermal venting at Vailulu'u Seamount: The smoking end of the Samoan chain, *Geochem. Geophys. Geosyst.*, *5*, Q02003, doi:10.1029/2003GC000626.

Tagliabue, A., et al. (2010), Hydrothermal contribution to the oceanic dissolved iron inventory, *Nat. Geosci.*, *3*(4), 252–256.

Trefry, J. H., and S. Metz (1989), Role of hydrothermal precipitates in the geochemical cycling of vanadium, *Nature*, *342*(6249), 531–533.

Wheat, G. C., R. A. Feely, and M. J. Mottl (1996), Phosphate removal by oceanic hydrothermal processes: An update of the phosphorus budget in the oceans, *Geochim. Cosmochim. Acta*, *60*(19), 3593–3608.

Yücel, M., A. Gartman, C. S. Chan, and G. W. Luther III (2011), Hydrothermal vents as a kinetically stable source of iron-sulphide-bearing nanoparticles to the ocean, *Nat. Geosci.*, *4*(6), 367–371.

HAWKES ET AL.   947